Journal of Materials Chemistry B

ROYAL SOCIETY OF CHEMISTRY

PAPER

View Article Online
View Journal | View Issue

Cite this: J. Mater. Chem. B, 2022, 10, 2637

Photoresponsive behaviour of zwitterionic polymer particles with photodimerizable groups on their surfaces†

Takashi Miyata, *[ab] Takayuki Namera,[a] Yihua Liu,[c] Akifumi Kawamura [ab] and Tetsuji Yamaoka [c]

Received 25th October 2021,
Accepted 3rd January 2022

DOI: 10.1039/d1tb02342j

rsc.li/materials-b

Polymer particles with precise diameters have been used as building blocks for fabricating well-defined and nanostructured materials. Polymer particles as building blocks for medical applications require both easily spatiotemporal manipulation and good biocompatibility. In this study, we designed zwitterionic polymer particles with photodimerizable groups on their surfaces and used ultraviolet (UV) light irradiation to photo-assemble them in aqueous media. After synthesizing zwitterionic polymer particles with diameters ranging from 100–200 nm *via* soap-free emulsion polymerization, maleimide moieties as photodimerizable groups were introduced onto the particle surfaces. UV light irradiation to an aqueous dispersion of zwitterionic polymer particles with photodimerizable groups induced their photo-assembling because interparticle bonding forms by photodimerization of the photodimerizable groups on the particle surfaces. The zwitterionic surface of their particle-assembled films effectively suppressed protein adsorption, cell adhesion, and platelet adhesion. The photoresponsive behaviour and bioinert surface of the zwitterionic polymer particles with photodimerizable groups indicate that they have several potential applications as bioinert building blocks for designing well-defined and nanostructured biomaterials used in biosensors, bioseparation and cell culture, and for modifying and repairing biomaterial surfaces *in situ*.

Introduction

Polymer particles with sizes ranging from nano to micro-meter scale dimensions are widely used in adhesives, cosmetics, inks, and paints, among other applications. In addition to their practical uses, various polymer particles have been studied as nano- and micro-tools for environmental, optical, electrical, and medical applications due to their large surface area and various surface functionalization.[1–5] Particularly, polymer particles with well-designed surfaces have several potential applications in drug delivery, bioseparation, and biosensing. Some polymer particles change in size or dispersibility in response to environmental changes, such as pH and temperature, as they change the hydrophilicity of their polymer chains.[6–9] In addition to such pH- and temperature-responsive polymer particles, a few photoresponsive polymer particles have been studied since light is a useful stimulus.[10–15] Changes in the volume of such stimuli-responsive polymer particles enable on/off regulation of drug release in response to a change in pH, temperature, and many others. Stimuli-responsive polymer particles that change from hydrophilic to hydrophobic properties in response to stimuli are well-dispersed in aqueous media without the stimuli but are aggregated and precipitated under stimuli. The fascinating properties of stimuli-responsive polymer particles can indicate that they have many future opportunities as suitable nanomaterials for self-regulated drug delivery, diagnostics, bioimaging, and separation of biomolecules and cells. However, these stimuli-responsive polymer particles have a few disadvantages in biomedical applications since changing the surface property from hydrophilic to hydrophobic induces protein adsorption and cell adhesion, implying that the particles become less bioinert.

Polymer particles with a predetermined diameter have also been used as building blocks for fabricating well-designed and nanostructured materials.[16–23] In the formation of nanostructured materials, polymer particles are self-assembled on substrates *via* general interactions such as electrostatic interactions, hydrogen bondings, and hydrophobic interactions. Self-assembly of polymer particles enables the spontaneous fabrication of well-designed and

[a] Department of Chemistry and Materials Engineering, Kansai University, 3-3-35, Yamate-cho, Suita, Osaka 564-8680, Japan. E-mail: tmiyata@kansai-u.ac.jp
[b] Organization for Research and Development of Innovative Science and Technology, Kansai University, 3-3-35, Yamate-cho, Suita, Osaka 564-8680, Japan
[c] Department of Biomedical Engineering, National Cerebral and Cardiovascular Center Research Institute, 6-1 Kishibe Shim-machi, Suita, Osaka 564-8565, Japan

† Electronic supplementary information (ESI) available. See DOI: 10.1039/d1tb02342j

nanostructured materials with large scales while requiring no additional energy and driving forces. However, since precise manipulation of polymer particles *via* only self-assembly is difficult, the design of stimuli-responsive particles that can be spatiotemporally assembled in response to a stimulus is necessary for fabricating more complicated and nanostructured materials. Light, unlike pH and temperature, is a remote stimulus that can be spatiotemporally regulated. By using light as a stimulus to manipulate polymer particles, well-designed materials with spatiotemporally-modulated nano- and macro-scale structures can be fabricated. Therefore, photoresponsive polymer particles whose assembling can be spatiotemporally regulated by light irradiation become essential tools as building blocks for fabricating well-designed and nanostructured materials. However, photoresponsive polymer particles for fabricating biomaterials for medical applications require not only photo responsiveness but also bioinert surfaces. General photoresponsive polymer particles that change in size and dispersibility in response to light irradiation are ineffective as building blocks for fabricating well-designed and nanostructured biomaterials because their surfaces become less bioinert due to a photoresponsive change from hydrophilic to hydrophobic.

Implantable biomaterials, such as artificial hearts and blood vessels are crucial in improving patients' quality of life. The surfaces of these implantable biomaterials are coated with bioinert polymers such as poly(ethylene glycol) (PEG) and poly(2-methacryloyloxyethyl phosphorylcholine) (PMPC).[24–30] Particularly, 2-methacryloyloxyethyl phosphorylcholine (MPC) is a zwitterionic monomer designed by bioinspiration of neutral and zwitterionic phosphorylcholine lipids such as phosphatidylcholines that when copolymerized with other monomers produces blood-compatible polymer materials with cell membrane-like surfaces. Various MPC-based polymers and surfaces have been designed for developing biomaterials and medical devices with excellent biointerfaces between artificial and biological systems. Some reports on the synthesis and medical applications of MPC-based polymer particles for bioseparation, diagnosis, and drug delivery have been reported because their bioinert surfaces suppress protein adsorption, cell adhesion, and so on.[31–34] Thus, the photoresponsive MPC-based polymer particles that are photo-assembled by light irradiation have numerous potential applications as building blocks for fabricating well-designed and nanostructured biomaterials. In addition, the photoresponsive MPC-based polymer particles may enable the modification of less bioinert surfaces or to repair scratched biomaterial surfaces *in situ* in aqueous media since they can be retained in the target region for a long time due to their lower diffusivity than MPC-based polymers.

We have synthesized various stimuli-responsive polymer materials such as hydrogels, films, and particles using dynamic crosslinks based on biomolecular or supramolecular complexes.[35–41] Our previous studies demonstrate that dynamic or responsive crosslinks provide useful tools for designing stimuli-responsive polymer materials. The concept of using responsive crosslinks can be applied to photoresponsive polymer particles assembled by light irradiation. We focused on photodimerization to form photoresponsive crosslinks between particles and to induce their spatiotemporal photo-assembling in response to light irradiation. In photodimerization, photodimerizable molecules, such as cinnamic acid, coumarin, and maleimide, are excited by light irradiation and form dimers with cyclobutane rings from olefin double bonds.[42] Our strategy for designing photoresponsive polymer particles that can be spatiotemporally assembled without changing their hydrophilicity by light irradiation is to introduce photodimerizable groups, which form interparticle bonds *via* photodimerization, onto polymer particles with bioinert surfaces (Fig. 1). In this study, we synthesized zwitterionic polymer particles with photodimerizable groups and investigated their photo-assembling behaviour in aqueous media and biocompatibility.

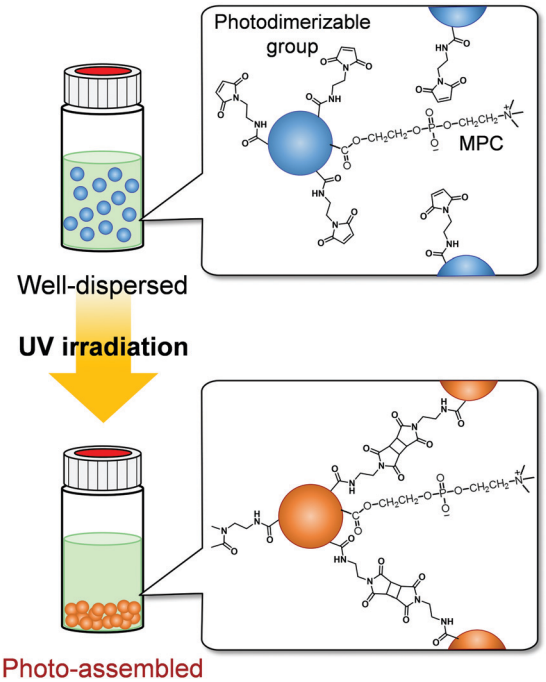

Fig. 1 Schematic representation of the photo-assembling behaviour of zwitterionic polymer particles with photodimerizable groups on their surfaces.

Experimental

Materials

Styrene (St), methacrylic acid (MAA), divinylbenzene (DVB), ammonium peroxodisulfate (APS), 1-ethyl-3-(3-dimethylaminopropyl) carbodiimide hydrochloride (EDC), and *N*-hydroxysuccinimide (NHS) were purchased from FUJIFILM Wako Pure Chemical Corporation (Osaka, Japan) and used as received. 2-Methacryloyloxyethyl phosphorylcholine (MPC) was provided by NOF Corporation (Tokyo, Japan). *N*-(2-Aminoethyl) maleimide hydrochloride (AEM), 4-maleimidobutylic acid, and 3-aminopropyltrimethoxysilane (APTMS) were purchased from Tokyo Chemical Industry Co., Ltd (Tokyo, Japan) and used as received. Bovine serum albumin labeled

with fluorescein isothiocyanate (FITC-BSA) was purchased from Sigma-Aldrich (St. Louis, USA). Formaldehyde (16%) was purchased from Polysciences Inc. (PA, USA). Eagle's minimal essential medium (EMEM) and phosphate-buffered saline (PBS(−)) were purchased from Nissui Pharmaceutical Co., Ltd (Tokyo, Japan). Fetal bovine serum (FBS) was purchased from Biowest (Nuaille, France). All aqueous solutions were prepared with ultrapure water (Milli-Q, 18.2 MΩ cm). Other solvents and reagents of analytical grade were obtained from commercial sources and were used without further purification.

Synthesis of zwitterionic polymer particles by soap-free emulsion polymerization

Zwitterionic polymer particles were synthesized *via* soap-free emulsion polymerization (Fig. 2). Table 1 summarizes the feed compositions for the synthesis of P(styrene-*co*-methacrylic acid-*co*-2-methacryloyloxyethyl phosphorylcholine) (P(St-*co*-MAA-*co*-MPC)) particles. Appropriate amounts of St, DVB, MAA, and MPC as monomers and APS as an initiator were added to 300 mL water in a three-necked round-bottom flask equipped with a condenser and a nitrogen inlet, and then the mixture was stirred for 6 h at 85 °C at 300 rpm under nitrogen atmosphere. The product appeared milky white after the reaction. The reaction mixture in which the resulting P(styrene-*co*-methacrylic acid) (P(St-*co*-MAA)) or P(St-*co*-MAA-*co*-MPC) particles were dispersed was centrifuged (rotational speed 12 000 rpm, 4 °C, 60 min) and the supernatant was decanted. This procedure was repeated three times to purify the resultant polymer particles.

Introduction of photodimerizable groups onto polymer particles

Maleimide moieties as photodimerizable groups were introduced onto the surface of P(St-*co*-MAA) and P(St-*co*-MAA-*co*-MPC) particles according to Fig. 3.[43] Table 2 summarizes the feed compositions for introducing maleimide moieties onto the particles. In a light-shielded round-bottom flask, two and five equivalents of AEM and MAA of the particles were respectively added to water-based particle dispersions together with EDC and NHS; the mixtures were stirred for 24 h at room temperature. In this study, neither acid nor alkali was used in introducing maleimide moieties onto the particles to avoid the hydrolysis of the polymer particles although the use of an acid or alkali enhances the efficiency of the reaction. After the reaction, the particle dispersions were centrifuged (rotational speed 12 000 rpm, 4 °C, 60 min) and the supernatant was decanted. This procedure was repeated three times to purify the resultant maleimide-P(St-*co*-MAA) and maleimide-P(St-*co*-MAA-*co*-MPC) particles.

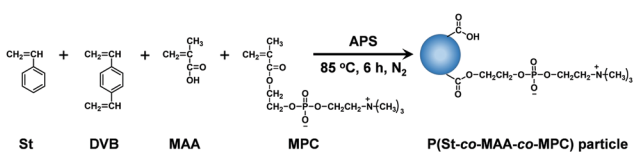

Fig. 2 Preparation of P(St-*co*-MAA-*co*-MPC) particles *via* soap-free emulsion polymerization.

Characterization of zwitterionic polymer particles

The diameters of P(St-*co*-MAA), P(St-*co*-MAA-*co*-MPC), maleimide-P(St-*co*-MAA), and maleimide-P(St-*co*-MAA-*co*-MPC) particles in water were measured *via* dynamic light scattering (DLS), using DLS-7000K (Otsuka Electronics Co., Ltd, Osaka, Japan). Vertically polarized light at 633 nm from the He–Ne-ion laser was used as the incident beam, and all measurements were performed at 25 °C ± 0.3 °C. The morphology of the particles was observed *via* scanning electron microscopy (SEM), using JSM-6700F (JEOL Ltd, Tokyo, Japan) at an accelerating voltage of 5.0 kV. To prepare samples for SEM observations, a diluted dispersion of particles was deposited on a silicon wafer and dried *via* lyophilization. Then, it was placed in a vacuum, evacuated, and a layer of platinum was deposited under flushing with nitrogen using JFC-1500 sputter coater (JEOL Ltd, Tokyo, Japan). The chemical structures of the particles were examined using the KBr method using a Fourier-transform infrared spectrometer (FT-IR) (Spectrum 100: PerkinElmer, Inc., MA, USA) after freeze-drying the particles. All the spectra represent an average of 32 scans taken in the wavenumber range of 450–4000 cm^{-1}.

X-Ray photoelectron spectroscopy (XPS) spectra were recorded using the ESCA-3400 (Shimadzu Co., Kyoto, Japan). A 150 W (15 mA × 10 kV) MgKα X-ray source was used with a pass energy of 75 eV. The pressure in the analysis chamber was *ca.* 4.0×10^{-7} Pa. The charge correction in the binding energy scale was performed by setting the $-CH_2-$ peak in the carbon spectra to 285.0 eV. The surface compositions (in atomic %) of particles were determined by considering the integrated peak areas of C_{1s}, N_{1s}, O_{1s}, and P_{2p} and their respective experimental sensitivity factors. The following experimental sensitivity factors were used: 1.000, 2.850, 1.770, and 1.250 for C_{1s}, O_{1s}, N_{1s}, and P_{2p}, respectively. The fractional concentration of a particular element A (%*A*) was computed using eqn (1):

$$\%A = \frac{I_A/s_A}{\sum (I_n/s_n)} \times 100 \quad (1)$$

where I_A and s_n are the integrated peak areas and sensitivity factors, respectively. Particles were placed on a silicon wafer and dried under reduced pressure before XPS measurements.

Photo-assembling behaviour in zwitterionic polymer particles

Aqueous dispersions of polymer particles with particle concentrations of 2.0 and 5.0 mg mL^{-1} and a NaCl concentration of 150 mM were prepared as samples to investigate the photo-responsive behaviour. The behaviour of the polymer particles in the dispersions was observed during their exposure to UV light at 270 nm (20 mW cm^{-2}) using MAX-303 (Asahi Spectra Co., Ltd, Tokyo, Japan). After UV irradiation for a predetermined period, the diameter of the particles was measured *via* DLS, using DLS-7000K (Otsuka Electronics Co., Ltd, Osaka, Japan). Vertically polarized light at 633 nm from the He–Ne ion laser

Table 1 Preparation conditions and diameters of P(St-*co*-MAA-*co*-MPC) particles

In feed							Particle	
MPC (mol%)	St (mmol)	DVB (mmol)	MMA (mmol)	MPC (mmol)	APS (mmol)	Water (mL)	Diameter[a] (nm)	PDI[a]
0	6.6	0.9	1.5	0	0.5	300	145	0.099
10	5.5	0.9	1.8	0.9	0.5	300	160	0.077
15	5.0	0.9	1.8	1.4	0.5	300	112	0.088

[a] Determined *via* DLS measurements in water at room temperature.

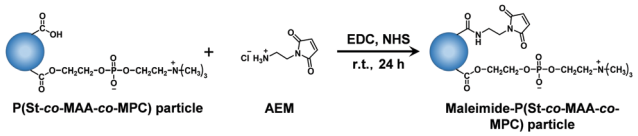

Fig. 3 Introduction of maleimide moieties onto the surface of P(St-*co*-MAA-*co*-MPC) particles.

was used as the incident beam, and all measurements were performed at 25 °C ± 0.3 °C.

In addition, particle dispersions were injected into a target region of a glass substrate in water using a micropipette, while UV light at 270 nm (20 mW cm^{-2}) using MAX-303 (Asahi Spectra Co., Ltd, Tokyo, Japan) was irradiated to the target area. It took only a few seconds to inject the particle dispersions into the target region in water. However, after the injection of the particle dispersion under UV irradiation, the target area of the glass substrate in water was kept exposed to UV light for 60 min. Before injecting the dispersions, the glass substrate was modified with maleimide as follows: After casting a toluene solution with 5 vol% APTMS on the cleaned glass substrate and heated at 70 °C for 6 h, the substrate was washed with toluene and ethanol.[44] On the amino group-introduced glass substrate, maleimide moieties were introduced by reacting 4-maleimidobutylic acid and amino groups using EDC and NHS for 24 h. We confirmed the successful surface modification of glass substrates with maleimide moieties using attenuated total reflection FT-IR (Spectrum 100: PerkinElmer, Inc., MA, USA) (Fig. S1, ESI†).

Protein adsorption on zwitterionic polymer particle-assembled films

First, maleimide-P(St-*co*-MAA) particle- and maleimide-P(St-*co*-MAA-*co*-MPC) particle-assembled films for investigating protein adsorption were prepared as follows: An aqueous dispersion of polymer particles was arranged at a predetermined particle concentration by adding water. Then, the polymer particle-assembled films were fabricated by casting the aqueous particle dispersion on silicon wafers or 24-well plates and drying them. The particle-assembled films were exposed to UV light with a wide wavelength of 250–400 nm (20 mW cm^{-2}) for 3 min using MAX-303 (Asahi Spectra Co., Ltd, Tokyo, Japan).

Protein adsorption on the particle-assembled films was evaluated as follows: After being immersed in PBS(−) overnight, the particle-assembled films were immersed in 5 mL of 0.2 mg mL^{-1} FITC-BSA/PBS(−) solution for 2 h. Afterward, the films were washed three times with PBS(−). A fluorescence microscope (IX71, Olympus corp., Tokyo, Japan) was used to observe the FITC-BSA adsorption on the particle-assembled films.

Cell adhesion on zwitterionic polymer particle-assembled films

Cell adhesion on the particle-assembled films was evaluated as follows: After the particle-assembled films were prepared on 24-well plates *via* the casting method, the films were exposed to UV light with a wide wavelength of 250–400 nm (20 mW cm^{-2}) for 5 min using MAX-303 (Asahi Spectra Co., Ltd, Tokyo, Japan). Then, the particle-assembled films were washed three times with ethanol and PBS(−) in a 24-well plate. Mouse fibroblasts (hereinafter, L929 cells) were seeded at 2.0×10^4 cells per well in a 24-well plate in EMEM containing 10% FBS. The cells were cultured in an incubator at 37 °C with 5% (v/v) CO_2 for 48 h and then rinsed three times with EMEM. A phase-contrast microscope (IX71, Olympus corp., Tokyo, Japan) was used to observe cell adhesion on the particle-assembled films after cell culture. In addition, after 48 h of culture, the number of cells adhered to the particle-assembled films was counted, and the average number of cells was calculated.

Platelet adhesion on zwitterionic polymer particle-assembled films

Platelet adhesion to the particle-assembled films was evaluated as follows: After the particle-assembled films were prepared on substrates by the casting method, the films were exposed to UV

Table 2 Preparation conditions and diameters of maleimide-P(St-*co*-MAA-*co*-MPC) particles

P(St-*co*-MAA-*co*-MPC) particles		Photodimerizable group	Condensation reagent		Maleimide-P(St-*co*-MAA-*co*-MPC) particles	
MPC (mol%)	MAA (mmol)	AEM (mmol)	EDC (mmol)	NHS (mmol)	Diameter[a] (nm)	PDI[a]
0	0.18	0.36	0.36	0.43	262	0.233
10	0.18	0.36	0.36	0.43	160	0.036
15	0.30	0.60	0.60	0.72	112	0.094

[a] Determined *via* DLS measurements in water at room temperature.

light with a wide wavelength of 250–400 nm (20 mW cm^{-2}) for 5 min using MAX-303 (Asahi Spectra Co., Ltd, Tokyo, Japan). Then, the particle-assembled films were washed three times with ethanol and PBS(−) and placed in a 24-well plate. 45 mL of fresh porcine whole blood was mixed in a 9 : 1 volume ratio with 5 mL of an acid citrate dextrose anticoagulant buffer (citric acid, 73 mg; tri-sodium citrate dihydrate, 220 mg; D(+)-glucose, 22 mg; H_2O, 10 mL). Platelet-rich plasma (PRP) was obtained by centrifugation at 600 g for 4 min, whereas platelet-poor plasma (PPP) was obtained by centrifugation at 1300 g for 10 min. The platelets were counted using a Beckman Coulter Z2 counter (Beckman Coulter Inc., CA, USA). The final platelet concentration was adjusted to 8×10^7 platelets per mL by mixing PRP with PPP. Each sample was fixed in a 24-well plate using a silicone ring to prevent them from floating and an 8 mm diameter metal ring was used to control the tested area. All samples were incubated with platelet suspension (2×10^7 platelets/250 μL per well) for 1 h at 37 °C under 5% CO_2. After washing the samples three times with PBS, the adhered platelets were fixed using 250 μL of 4% formaldehyde in PBS for 10 min. The platelets were treated with 250 μL of 0.1% Triton X-100 in PBS after being washed three times with PBS. Further, the samples were again washed three times with PBS after 3 min and stained with 250 μL per well of 1/40 (v/v) rhodamine phalloidin in PBS for 30 min in the dark. The resultant samples, after being washed three times using PBS, were mounted on glass plates with a drop of mounting medium (Fluoro-keeper antifade reagent, nonhardening type) and sealed using nail polish before confocal laser scanning microscopy (CLSM) (FV1000-D, Olympus, Tokyo, Japan).[45–47] The morphologies of the platelets adhered to the particle-assembled films were visualized using SEM (Carry Scope JCM-5700, JEOL Technology Ltd, Japan). After the adhered platelets were fixed on the samples using formaldehyde and rinsed three times using PBS, they were dehydrated in EtOH aqueous mixtures of increasing concentrations (50, 60, 70, 80, 90, and 100% EtOH) for 10 min each. The samples were finally dried under vacuum and then coated with gold using an ion sputtering coater (IB3, Giko, Engineering Co., Tokyo, Japan) before the SEM observation.

Results and discussion

Synthesis and characterization of zwitterionic polymer particles with photodimerizable groups

Emulsion polymerization is an effective method for preparing submicron-sized polymer particles. Surfactants are used in standard emulsion polymerization to stabilize and disperse monomer emulsions and the resulting polymer particles in aqueous media. Residue surfactants on the surface of the resulting polymer particles negatively impact their properties and functions, such as biocompatibility. However, removing the surfactants from the surface of the polymer particles is challenging due to the strong hydrophobic interactions. We can prepare polymer particles with a clean surface using soap-free emulsion polymerization.[48–55] Using soap-free emulsion polymerization, we have designed various stimuli-responsive particles that exhibit rapid size changes in response to pH, reduction environment, glucose, and so on.[56,57] In this study, we applied soap-free emulsion polymerization to prepare zwitterionic polymer particles with clean surfaces. St, MAA, and MPC were chosen as a hydrophobic monomer for forming a hydrophobic core, a functional monomer for the introduction of photodimerizable groups, and a zwitterionic monomer for stabilizing the resulting particles in aqueous media and forming a bioinert surface, respectively. Table 1 shows the conditions for the soap-free emulsion copolymerization, size, and polydispersity index (PDI) of the resulting P(St-*co*-MAA-*co*-MPC) particles, which were determined *via* DLS measurements. The DLS measurements demonstrate that P(St-*co*-MAA) and P(St-*co*-MAA-*co*-MPC) particles with a diameter of 100–160 nm were successfully synthesized using soap-free emulsion polymerization.

SEM image in Fig. S2 (ESI†) demonstrates that the P(St-*co*-MAA-*co*-MPC) particles with an MPC content of 10 mol% had spherical shapes. The diameter was a little smaller than that determined from the DLS measurement because the sample for SEM observation was dried. In general, hydrophobic and hydrophilic polymer chains are preferentially concentrated in the core and at the surface of the particle, respectively. Therefore, we think that hydrophilic MAA and MPC had preferentially concentrated near the surface of the zwitterionic polymer particle. Namely, the zwitterionic polymer particles had a hairy structure with hydrophilic polymer chains containing rich MAA and MPC, which were swollen in aqueous media, and with a hydrophobic core containing rich St and DVB, which was not swollen. In the case of such polymer particles with a hairy structure, the size of the dried particles determined from SEM observation is significantly smaller than that determined from the DLS, which is calculated as the hydrodynamic radius, due to the shrinkage of the hairy structure. Thus, the DLS measurements and SEM observations suggest the successful formation of sphere particles with a diameter of 100–160 nm and a narrow size distribution.

Further, we used FT-IR and XPS measurements to characterize the chemical structure of the P(St-*co*-MAA-*co*-MPC) particles. Fig. S3 (ESI†) shows the FT-IR spectra of P(St-*co*-MAA) and P(St-*co*-MAA-*co*-MPC) particles with an MPC content of 10 mol%. In the FT-IR spectrum of the P(St-*co*-MAA-*co*-MPC) particles, a peak at 1200 cm^{-1} was assigned to the P=O stretching vibrations based on the phosphate ester of MPC, which was not observed in the spectrum of the P(St-*co*-MAA) particles. These results indicate that the (St-*co*-MAA-*co*-MPC) particles have a zwitterionic MPC chain, unlike the (St-*co*-MAA) particles.

Fig. 4 shows XPS spectra of N_{1s} and P_{2p} regions of P(St-*co*-MAA-*co*-MPC) and P(St-*co*-MAA) particles. P(St-*co*-MAA-*co*-MPC) particles had a higher peak in the N_{1s} spectrum than P(St-*co*-MAA) particles. The peak in the N_{1s} spectrum of P(St-*co*-MAA-*co*-MPC) particles at 403 eV was attributed to the quaternary amine of MPC, and a small peak around 400 eV in the N_{1s} spectrum of

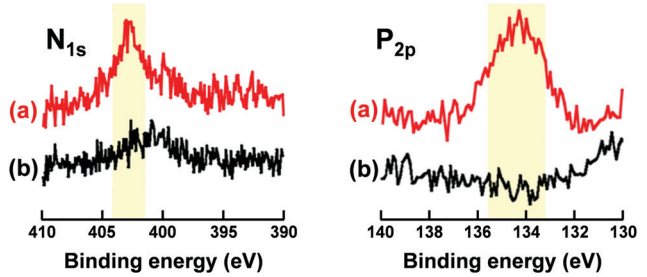

Fig. 4 XPS spectra of N_{1s} and P_{2p} region of (a) P(St-*co*-MAA-*co*-MPC) particles with an MPC content of 10 mol% and (b) P(St-*co*-MAA) particles.

P(St-*co*-MAA) particles may be attributed to the initiator APS introduced into the terminal of polymer chains. A distinct peak was observed around 134 eV in the P_{2p} spectrum of the P(St-*co*-MAA-*co*-MPC) particles, whereas no peak was observed in the P_{2p} spectrum of the P(St-*co*-MAA) particles. Table S1 (ESI†) summarizes the atomic ratios of the surfaces of P(St-*co*-MAA-*co*-MPC) and P(St-*co*-MAA) particles determined *via* XPS measurements. The surface of P(St-*co*-MAA-*co*-MPC) particles with an MPC content of 10 mol% had a higher atomic ratio of N_{1s} and P_{2p} than that of P(St-*co*-MAA) particles. These indicate that the P(St-*co*-MAA-*co*-MPC) particles have a zwitterionic MPC chain on the surface. The zwitterionic MPC chain on the surface allows the proper dispersion of P(St-*co*-MAA-*co*-MPC) particles in aqueous media.

To prepare zwitterionic polymer particles with photodimerizable groups, we introduced maleimide moieties onto the surfaces of P(St-*co*-MAA-*co*-MPC) and P(St-*co*-MAA) particles *via* condensation between an amino group of AEM and carboxy group of MAA components of the particle surface. Table 2 shows the diameter and PDI of the resulting maleimide-P(St-*co*-MAA-*co*-MPC) and maleimide-P(St-*co*-MAA) particles determined *via* DLS measurements. The maleimide-P(St-*co*-MAA-*co*-MPC) particles maintained a particle size of 100–160 nm and a low PDI, whereas both diameter and PDI of the maleimide-P(St-*co*-MAA) particles were greater than P(St-*co*-MAA) particles. The introduction of maleimide moieties increases the diameter and PDI of P(St-*co*-MAA) particles, which is attributed to a change from a hydrophilic carboxy group of MAA to a hydrophobic maleimide moiety. However, the maleimide-P(St-*co*-MAA-*co*-MPC) particles were stably dispersed in water without aggregation because the zwitterionic MPC chain stabilizes the particle surface by excluded volume of the hydrophilic polymer chains in aqueous media.

XPS measurements were used to characterize the chemical structure of the particles after the introduction of maleimide moieties onto their surfaces. Fig. S4 (ESI†) demonstrates a significant difference in the N_{1s} spectrum between the P(St-*co*-MAA-*co*-MPC) particles before and after MAA and AEM reactions. Table 3 shows the atomic ratios of C_{1s}, O_{1s}, N_{1s}, and P_{2p} of maleimide-P(St-*co*-MAA-*co*-MPC) and P(St-*co*-MAA-*co*-MPC) particles obtained *via* XPS measurements. The atomic ratio of nitrogen in the maleimide-P(St-*co*-MAA-*co*-MPC) particles increased compared to that in the P(St-*co*-MAA-*co*-MPC) particles. The carboxy groups might

Table 3 Atomic ratio of P(St-*co*-MAA-*co*-MPC) and maleimide-P(St-*co*-MAA-*co*-MPC) particles

Atomic ratio (%)	P(St-*co*-MAA-*co*-MPC)	Maleimide-P (St-*co*-MAA-*co*-MPC)
C_{1s}	77.2	79.7
O_{1s}	20.4	17.3
N_{1s}	0.9	2.0
P_{2p}	0.9	1.1

be preferentially distributed near the surface of the particles for lowering the interfacial free energy in aqueous media. Therefore, AEM with a maleimide moiety can more effectively react with carboxy groups near the surface of the particles than those in their core because the amount of the former carboxy groups is larger than that of the latter. In addition, AEM is difficult to react with the carboxy groups inside the particles because of its lower diffusivity in the crosslinked and unswollen core of the particles. These results indicate the successful synthesis of maleimide-P(St-*co*-MAA-*co*-MPC) particles with zwitterionic polymer chains and photodimerizable moieties on their surfaces.

Photo-assembling of maleimide-P(St-*co*-MAA-*co*-MPC) particles

As described in the previous section, maleimide-P(St-*co*-MAA-*co*-MPC) particles were successfully synthesized as zwitterionic polymer particles with photodimerizable groups at the surface, which were well-dispersed in aqueous media. Further, we investigated the photoresponsive behaviour of the maleimide-P(St-*co*-MAA-*co*-MPC) particles with an MPC content of 15 mol% well-dispersed in aqueous media. Fig. 5 shows photographs of P(St-*co*-MAA-*co*-MPC) and maleimide-P(St-*co*-MAA-*co*-MPC)

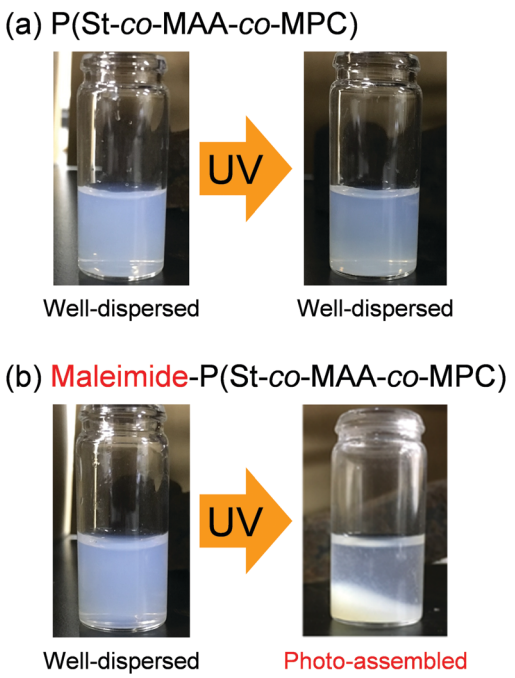

Fig. 5 Photographs of (a) P(St-*co*-MAA-*co*-MPC) and (b) maleimide-P(St-*co*-MAA-*co*-MPC) particles in an aqueous solution of 150 mM NaCl before and after UV irradiation for 300 min.

particles in an aqueous solution with 150 mM NaCl, which is similar to the concentration in human blood, before and after UV irradiation for 300 min. The P(St-*co*-MAA-*co*-MPC) and maleimide-P(St-*co*-MAA-*co*-MPC) particles were well-dispersed at a particle concentration of 2.0 mg mL^{-1} in an aqueous NaCl solution before UV irradiation. Although general polymer particles may aggregate in aqueous solutions with high ionic strength, the hydrophilic and zwitterionic MPC chains on the particle surface are responsible for the good dispersibility of P(St-*co*-MAA-*co*-MPC) and maleimide-P(St-*co*-MAA-*co*-MPC) particles in aqueous NaCl solution. The P(St-*co*-MAA-*co*-MPC) particles without photodimerizable groups at the surface did not affect the good dispersibility in the aqueous NaCl solution after UV irradiation. Alternatively, the UV irradiation of maleimide-P(St-*co*-MAA-*co*-MPC) particles resulted in their aggregation and precipitation (Video S1). This implies that maleimide-P(St-*co*-MAA-*co*-MPC) particles are photo-assembled due to the photodimerization of the maleimide moieties on the particle surface.[42]

We measured the size of P(St-*co*-MAA-*co*-MPC) and maleimide-P(St-*co*-MAA-*co*-MPC) particles well-dispersed in an aqueous NaCl solution as a function of UV irradiation time to investigate the photo-assembling of maleimide-P(St-*co*-MAA-*co*-MPC) particles. Fig. 6 shows the relationship between UV irradiation time and diameter of the P(St-*co*-MAA-*co*-MPC) and maleimide-P(St-*co*-MAA-*co*-MPC) particles exposed to UV light. The size of P(St-*co*-MAA-*co*-MPC) particles did not change after UV irradiation for 360 min. However, the size of maleimide-P(St-*co*-MAA-*co*-MPC) particles increased gradually as the UV irradiation time increased. Polydispersity Index (PDI) is also a very important factor for evaluating the dispersibility and stability of polymer particles in aqueous media. As shown in Fig. S5 (ESI†), the PDI of P(St-*co*-MAA-*co*-MPC) particles without photodimerization groups remained below 0.1 and monodisperse even after UV irradiation, whereas that of maleimide-P(St-*co*-MAA-*co*-MPC) particles with photodimerization groups increased rapidly above 0.1 and became polydisperse. Therefore, the increase in the diameter of the maleimide-P(St-*co*-MAA-*co*-MPC) particles is attributed to the interparticle bonding induced by the photodimerization of maleimide moieties on the particle surface, resulting in the aggregation and precipitation of the particles by the photo-assembling. Although maleimide moieties on the maleimide-P(St-*co*-MAA-*co*-MPC) particles might undergo photodimerization within a particle, namely intraparticle photodimerization, it can induce no aggregation and precipitation of the particles because of no change in hydrophilicity of their surface and stability in aqueous media. Therefore, we can conclude that their photo-assembling behaviour is mainly induced by the photodimerization of the maleimide moieties between particles, namely interparticle photodimerization. In addition, as shown in Fig. S6 (ESI†), the maleimide-P(St-*co*-MAA-*co*-MPC) particles exhibited no change in the diameter in water without NaCl after UV irradiation. The ionic strength of aqueous media influences the hydration of the surface of polymer particles strongly. Therefore, we conclude that the photo-assembling behaviour of the maleimide-P(St-*co*-MAA-*co*-MPC) particles depends on the hydration of their surface in aqueous media.

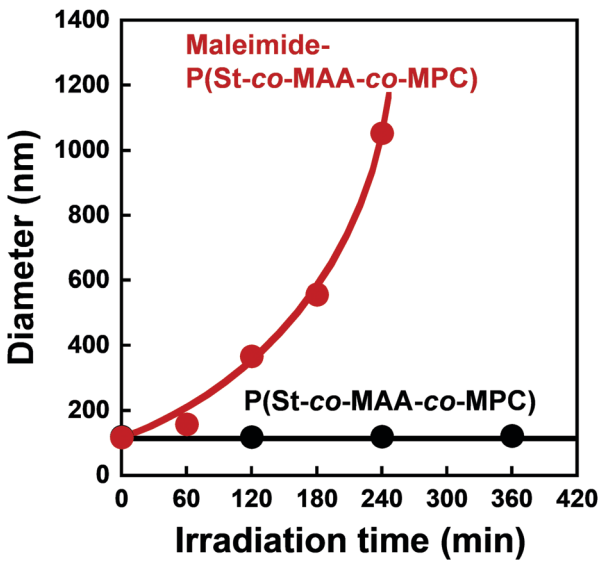

Fig. 6 Relationship between UV irradiation time and diameter of P(St-*co*-MAA-*co*-MPC) and maleimide-P(St-*co*-MAA-*co*-MPC) particles in an aqueous solution with 150 mM NaCl.

Photoresponsive polymer particles reported previously change in size and dispersibility in response to light irradiation because the hydrophilicity of the constituent polymer chains changes drastically by photoisomerization of the photoresponsive moieties such as azobenzene, spiropyran, and so on. While such photoresponsive polymer particles are well-dispersed in aqueous media, light irradiation causes them to aggregate and precipitate due to hydrophobic interaction or a decrease in aqueous media stability. When such photoresponsive polymer particles are photo-assembled by light irradiation, the change in the hydrophilicity of the particle surface significantly affects biocompatibility. Changes in the chemical properties of the particles from hydrophilic to hydrophobic often induce non-specific adsorption of proteins and cells, thereby lowering biocompatibility. Alternatively, the maleimide-P(St-*co*-MAA-*co*-MPC) particles are photo-assembled *via* interparticle bonding induced by photodimerization of maleimide moieties, even though the hydrophilicity of the particle surface remains unchanged. These results indicate that the maleimide-P(St-*co*-MAA-*co*-MPC) particles are photoresponsive with hydrophilic surfaces.

The maleimide-P(St-*co*-MAA-*co*-MPC) particles, unlike bioinert linear polymers, can be retained in the target region in aqueous media for a long time due to their lower diffusivity than linear polymers. Therefore, the maleimide-P(St-*co*-MAA-*co*-MPC) particles may enable us to modify the surface or repair scratched surface *in situ* in aqueous media using their photo-assembling properties. In this study, we also investigated the photo-assembling behaviour of maleimide-P(St-*co*-MAA-*co*-MPC) particles when they were injected into a target region of the substrate surface with and without maleimide moieties in

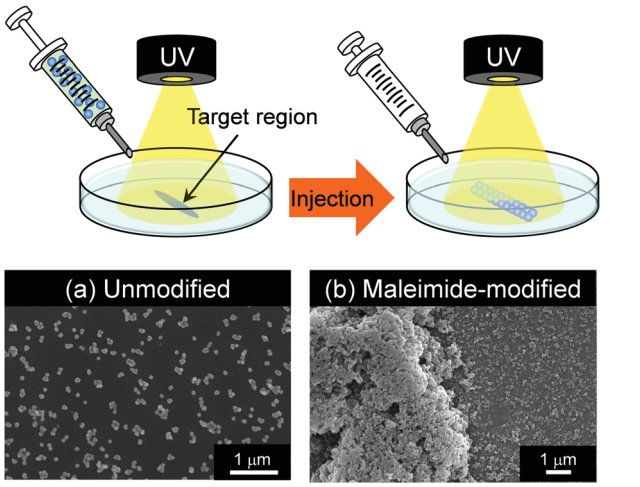

Fig. 7 SEM images of photo-assemblies of maleimide-P(St-*co*-MAA-*co*-MPC) particles on (a) unmodified and (b) maleimide-modified glass substrates after the particles were injected into the substrate surface under UV irradiation.

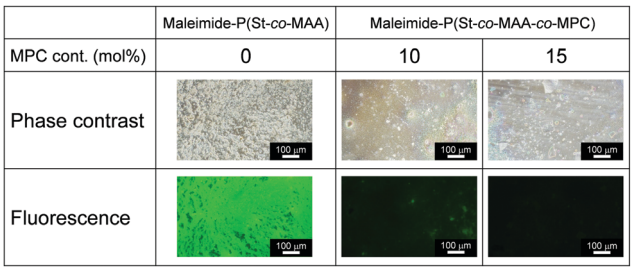

Fig. 8 Phase-contrast and fluorescence images of maleimide-P(St-*co*-MAA) particle- and maleimide-P(St-*co*-MAA-*co*-MPC) particle-assembled films after the adsorption of FITC-BSA 37 °C for 2 h.

aqueous media under UV irradiation. Fig. 7 shows that when 200 μL maleimide-P(St-*co*-MAA-*co*-MPC) particle dispersion with a particle concentration of 5.0 mg mL^{-1} was injected into the unmodified glass substrate's surface in an aqueous NaCl solution under UV irradiation, few particles were scattered on the substrate's surface and no particle-assembly was observed. On the other hand, SEM images demonstrate that particle assemblies were formed on a target region of the maleimide-modified glass substrate's surface in an aqueous NaCl solution under UV irradiation. This is due to both rapid photodimerization between the maleimide-P(St-*co*-MAA-*co*-MPC) particles and maleimide-modified glass substrate and interparticle bonding between the particles by UV irradiation. Although this is still a primitive result, the photo-assembling of maleimide-P(St-*co*-MAA-*co*-MPC) particles can be spatiotemporally manipulated using UV irradiation. This implies that the maleimide-P(St-*co*-MAA-*co*-MPC) particles have potential applications in embolization of aneurysms or in embolotherapy in which the flow of blood to a tumour is blocked. Even though the photo-assembling of maleimide-P(St-*co*-MAA-*co*-MPC) particles require further research into their potential applications for *in situ* surface modification and repair in aqueous media, they can be crucial biomaterials in the future.

Biocompatibility of maleimide-P(St-*co*-MAA-*co*-MPC) particle-assembled films

Medical applications of polymeric materials require the design of bioinert surfaces that suppress protein adsorption, cell adhesion, platelet adhesion, and so on. Zwitterionic MPC-based polymers have been widely used to design biomaterials and biodevices with bioinert surfaces. Because maleimide-P(St-*co*-MAA-*co*-MPC) particles have zwitterionic MPC chains on their surfaces, they could be used as photoresponsive building blocks in UV-irradiated assemblies and films. We studied protein adsorption and cell adhesion onto the films formed from maleimide-P(St-*co*-MAA-*co*-MPC) particles by UV irradiation to evaluate their potentials in medical applications.

The maleimide-P(St-*co*-MAA) and maleimide-P(St-*co*-MAA-*co*-MPC) particles were assembled by casting an aqueous dispersion, in which the particles were well-dispersed, on a silicon wafer. The particle-assembled films were prepared after exposing them to UV light for a few minutes. UV exposure resulted in the formation of stable particle-assembled films that were not dissociated in aqueous media because interparticle bonds were formed by the photodimerization of the maleimide moieties on the particle surface. Fluorescence microscopy revealed the adsorption of fluorescein-modified protein (FITC-BSA) onto the maleimide-P(St-*co*-MAA) particle- and maleimide-P(St-*co*-MAA-*co*-MPC) particle-assembled films. Fig. 8 shows that strong fluorescence derived from FITC-BSA was observed on the maleimide-P(St-*co*-MAA) particle-assembled film, but the fluorescence intensity on the maleimide-P(St-*co*-MAA-*co*-MPC) particle-assembled film decreased drastically as the MPC content increased. Surprisingly, no fluorescence was observed on the maleimide-P(St-*co*-MAA-*co*-MPC) particle-assembled film with an MPC content of 15 mol%. Because the maleimide-P(St-*co*-MAA) particle-assembled film lacks an MPC chain, a substantial amount of FITC-BSA was adsorbed onto its surface by hydrophobic interaction. Alternatively, the introduction of an MPC chain to the particles prevented FITC-BSA from adsorbing to the maleimide-P(St-*co*-MAA-*co*-MPC) particle-assembled film's surface. In general, protein adsorption onto polymer particles is strongly influenced by the hydrophilicity/hydrophobicity and charge of their surfaces.[58–60] Zwitterionic MPC-based polymers suppress nonspecific protein adsorption because their chains are extremely hydrophilic and neutral, and hydrated with water molecules having a specific state.[24,31,34] Therefore, the lack of FITC-BSA adsorption onto the maleimide-P(St-*co*-MAA-*co*-MPC) particle-assembled film is based on the zwitterionic MPC chain on the particle surface. This implies that the maleimide-P(St-*co*-MAA-*co*-MPC) particle-assembled films have bioinert surfaces due to the zwitterionic MPC chains on their surfaces. In addition, from the result that weak and no fluorescences were observed on maleimide-P(St-*co*-MAA-*co*-MPC) particle-assembled film with an MPC content of 10 mol% and 15 mol%, respectively, we conclude that the MPC content of more than 15 mol% is necessary to prepare

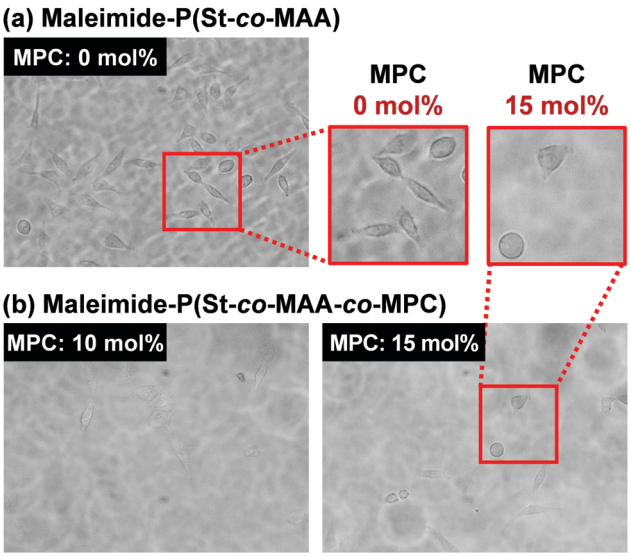

Fig. 9 Phase-contrast images of maleimide-P(St-*co*-MAA) particle- and maleimide-P(St-*co*-MAA-*co*-MPC) particle films after L929 cells were cultured on the films 37 °C for 2 days.

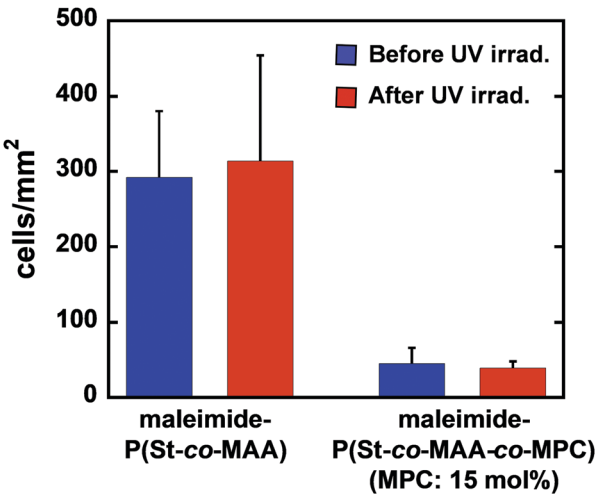

Fig. 10 Number of L929 cells adhered onto maleimide-P(St-*co*-MAA) and maleimide-P(St-*co*-MAA-*co*-MPC) particle-assembled films before and after UV irradiation.

the maleimide-P(St-*co*-MAA-*co*-MPC) particles with a bioinert surface.

Fig. 9 shows phase-contrast images of the maleimide-P(St-*co*-MAA) particle- and maleimide-P(St-*co*-MAA-*co*-MPC) particle-assembled films after L929 cells were cultured on the film surface at 37 °C for 2 days. The number of L929 cells adhered on the maleimide-P(St-*co*-MAA) particle-assembled film was higher than that on the maleimide-P(St-*co*-MAA-*co*-MPC) particle-assembled films with a 10 and 15 mol% MPC content. Interestingly, L929 cells were spread on the maleimide-P(St-*co*-MAA) particle-assembled film, but not on the maleimide-P(St-*co*-MAA-*co*-MPC) particle-assembled films. This implies that L929 cells strongly adhered to the maleimide-P(St-*co*-MAA) particle-assembled film, but only a few cells weakly adhered to the maleimide-P(St-*co*-MAA-*co*-MPC) particle-assembled films. Fig. 10 shows the number of L929 cells adhered to the maleimide-P(St-*co*-MAA) and maleimide-P(St-*co*-MAA-*co*-MPC) particle-assembled films before and after UV irradiation. The number of L929 cells adhered to the maleimide-P(St-*co*-MAA-*co*-MPC) particle-assembled film was reduced to about one-tenth of the maleimide-P(St-*co*-MAA) particle-assembled film. Notably, the number of L929 cells on the maleimide-P(St-*co*-MAA-*co*-MPC) particle-assembled film was unaffected by UV irradiation. Photoresponsive changes in hydrophilicity significantly influence protein adsorption and cell adhesion onto photoresponsive polymer particles that change in size or dispersibility in response to light irradiation. However, Fig. 10 demonstrates that photoresponsive interparticle bonding of the maleimide-P(St-*co*-MAA-*co*-MPC) particles by photodimerization of the maleimide moieties does not affect the L929 cell adhesion. Maleimide-P(St-*co*-MAA-*co*-MPC) particles, unlike general photoresponsive polymer particles, can only change their assembling behaviour under UV irradiation without affecting their surface chemical properties, such as hydrophilicity/hydrophobicity. Thus, UV irradiation on maleimide-P(St-*co*-MAA-*co*-MPC) particles does not affect cell adhesion.

Surface modifications using MPC-based polymers can improve blood compatibility by inhibiting protein adsorption and cell adhesion.[24,31,34] We investigated *in vitro* platelet adhesion onto the film before and after UV irradiation to further evaluate the maleimide-P(St-*co*-MAA-*co*-MPC) particle-assembled film's biocompatibility. Fig. 11 shows CLSM images of the platelets adhered to the maleimide-P(St-*co*-MAA) and maleimide-P(St-*co*-MAA-*co*-MPC) particle-assembled films before and after UV irradiation when the platelets were incubated on their films at 37 °C for an hour. Many platelets adhered to the maleimide-P(St-*co*-MAA) particle-assembled film before and after the UV irradiation. However, the number of platelets that adhered to the maleimide-P(St-*co*-MAA-*co*-MPC) particle-assembled film before and after UV irradiation was

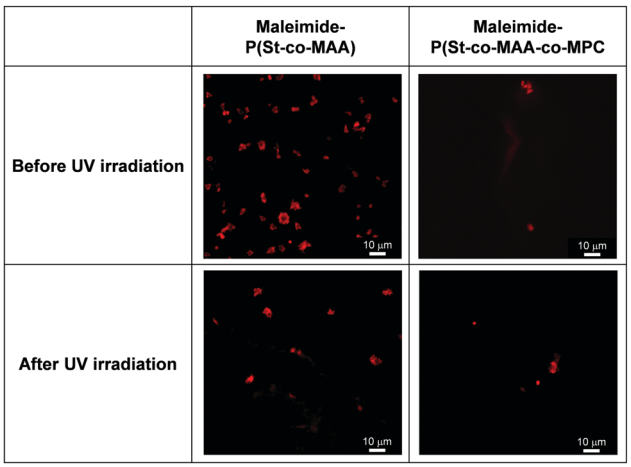

Fig. 11 CLSM images of platelets adhered to maleimide-P(St-*co*-MAA) and maleimide-P(St-*co*-MAA-*co*-MPC) particle-assembled films before and after UV irradiation.

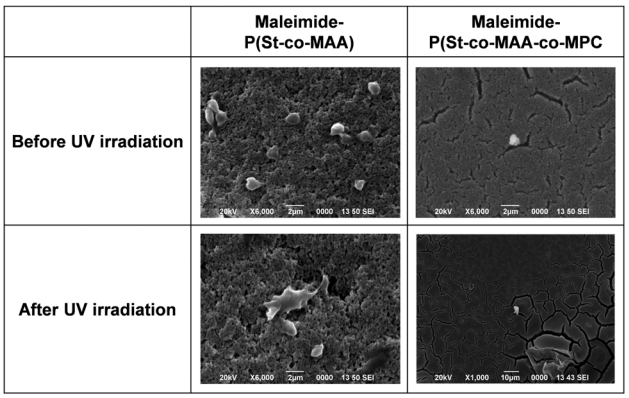

Fig. 12 SEM images of platelets adhered to maleimide-P(St-*co*-MAA) and maleimide-P(St-*co*-MAA-*co*-MPC) particle-assembled films before and after UV irradiation.

significantly few. Further, we observed the morphology of platelets adhered to their particle-assembled films using SEM. SEM images in Fig. 12 demonstrate that the number of platelets adhered to the maleimide-P(St-*co*-MAA-*co*-MPC) particle-assembled film was smaller than that on the maleimide-P(St-*co*-MAA) particle-assembled film. Activated and spread platelets were observed on the maleimide-P(St-*co*-MAA) particle-assembled film. Alternatively, the platelets on the maleimide-P(St-*co*-MAA-*co*-MPC) particle-assembled film exhibited a resting round shape, implying that few platelets were activated. These observations indicate that the MPC chains of the maleimide-P(St-*co*-MAA-*co*-MPC) particles suppress platelet adhesion. These can be supported by the results of FITC-BSA adsorption and L929 cell adherence to their films. The maleimide-P(St-*co*-MAA-*co*-MPC) particles' interparticle bonding did not affect platelet adhesion. This is because the hydrophilicity of the surface of the particles and assembled films did not change after the maleimide moieties were photodimerized. Thus, we conclude that the surface of the maleimide-P(St-*co*-MAA-*co*-MPC) particles can suppress protein adsorption and cell/platelet adhesion due to the zwitterionic MPC chain, even though they are photo-assembled by UV irradiation. The maleimide-P(St-*co*-MAA-*co*-MPC) particles may be useful building blocks for designing bioinert films and modifying the surface of substrates *in situ* because the maleimide-P(St-*co*-MAA-*co*-MPC) particles have some advantages as smart building blocks compared with standard zwitterionic polymers or photoresponsive polymers. For example, it is possible to accumulate the zwitterionic polymer particles on the surface of a substrate *in situ* in water, as shown in Fig. 7. Such *in situ* accumulation of the photoresponsive polymers is difficult in aqueous media because the diffusivity of the photoresponsive polymers is much greater than that of photoresponsive particles. Therefore, the maleimide-P(St-*co*-MAA-*co*-MPC) particles have several potential applications as smart biomaterials since they have both a bioinert MPC chain and a photo-assembling property. To the best of our knowledge, this is the first report on photo-assembling polymer particles with bioinert surfaces. Although the photoresponsive behaviour of zwitterionic polymer particles requires further research into their potential applications, they can be crucial bionanomaterials as photoresponsive building blocks for designing bioinert films, modifying device surfaces, and repairing defects of biomaterials *in situ* by UV irradiation.

Conclusions

Maleimide-P(St-*co*-MAA-*co*-MPC) particles were synthesized as zwitterionic polymer particles with both photodimerizable groups and bioinert MPC chains. DLS, SEM, and XPS measurements demonstrated that they were spherical particles with a diameter of 100–200 nm. When an aqueous dispersion with maleimide-P(St-*co*-MAA-*co*-MPC) particles was exposed to UV light, they were photo-assembled by interparticle bonding based on the photodimerization of maleimide moieties on their surfaces. FITC-BSA adsorption, L929 cell adhesion, and platelet adhesion on the particle-assembled films were investigated to evaluate the biocompatibility of maleimide-P(St-*co*-MAA-*co*-MPC) particles. Whereas a significant amount of FITC-BSA was adsorbed and L929 cells and platelets adhered on maleimide-P(St-*co*-MAA) particle-assembled films without an MPC chain, FITC-BSA adsorption, L929 cell adhesion, and platelet adhesion were not observed on maleimide-P(St-*co*-MAA-*co*-MPC) particle-assembled films before and after UV irradiation. MPC chains on the surface of the maleimide-P(St-*co*-MAA-*co*-MPC) particle-assembled films were critical in suppressing protein adsorption and cell adhesion. These findings indicate that maleimide-P(St-*co*-MAA-*co*-MPC) particles can be used as photoresponsive building blocks for fabricating well-designed and nanostructured biomaterials, as well as modifying and repairing surface and defects of biomaterials *in situ*.

Conflicts of interest

The authors declare no competing financial interest.

Acknowledgements

This work was supported by JSPS KAKENHI Grant Numbers No. JP20H04539 and No. JP20H05236 from the Japan Society for the Promotion of Science (JSPS), by the S-innovation Research Project of Japan Agency for Medical Research and Development (AMED), and by research grants from the Canon Foundation.

Notes and references

1 R. Shenhar, T. B. Norsten and V. M. Rotello, Polymer-mediated nanoparticle assembly: Structural control and applications, *Adv. Mater.*, 2005, **17**, 657–669.
2 W. H. De Jong and P. J. A. Borm, Drug delivery and nanoparticles: Applicatins and hazards, *Int. J. Nanomed.*, 2008, **3**, 133–149.

3 Y. Lu and M. Ballauff, Thermosensitive core–shell microgels: From colloidal model systems to nanoreactors, *Prog. Polym. Sci.*, 2011, **36**, 767–792.
4 J. Ramos, J. Forcada and R. Hidalgo-Alvarez, Cationic polymer nanoparticles and nanogels: From synthesis to biotechnological applications, *Chem. Rev.*, 2014, **114**, 367–428.
5 S. Jung, J. L. Kaar and M. P. Stoykovich, Design and functionalization of responsive hydrogels for photonic crystal biosensors, *Mol. Syst. Des. Eng.*, 2016, **1**, 225–241.
6 O. J. Cayre, N. Chagneux and S. Biggs, Stimulus responsive core-shell nanoparticles: synthesis and applications of polymer based aqueous systems, *Soft Matter*, 2011, **7**, 2211–2234.
7 M. I. Gibson and R. K. O'Reilly, To aggregate, or not to aggregate? considerations in the design and application of polymeric thermally-responsive nanoparticles, *Chem. Soc. Rev.*, 2013, **42**, 7204–7213.
8 M. Karimi, A. Ghasemi, P. S. Zangabad, R. Rahighi, S. M. M. Basri, H. Mirshekari, G. M. Amiri, Z. S. Pishabad, A. Aslani, M. Bozorgomid, D. Ghosh, A. Beyzavi, A. Vaseghi, A. R. Aref, L. Haghani, S. Bahrami and M. R. Hamblin, Smart micro/nanoparticles in stimulus-responsive drug/gene delivery systems, *Chem. Soc. Rev.*, 2016, **45**, 1457–1501.
9 X. Fu, L. Hosta-Rigau, R. Chandrawati and J. Cui, Multi-stimuli-responsive polymer particles, films, and hydrogels for drug delivery, *Chem*, 2018, **4**, 2084–2107.
10 P. K. Kundu, D. Samanta, R. Leizrowice, B. Margulis, H. Zhao, M. Börner, T. Udayabhaskararao, D. Manna and R. Klajn, Light-controlled self-assembly of non-photoresponsive nanoparticles, *Nat. Chem.*, 2015, **7**, 646–652.
11 E. R. Ruskowitz and C. A. DeForest, Photoresponsive biomaterials for targeted drug delivery and 4D cell culture, *Nat. Rev. Mater.*, 2018, **3**, 17087.
12 A. Abdollahi, K. Sahandi-Zangabad and H. Roghani-Mamaqani, Rewritable anticounterfeiting polymer inks based on functionalized stimuli-responsive latex particles containing spiropyran photoswitches: reversible photopatterning and security marking, *ACS Appl. Mater. Interfaces*, 2018, **10**, 39279–39292.
13 G. Li, H. Wang, Z. Zhu, J.-B. Fan, Y. Tian, J. Meng and S. Wang, Photo-irresponsive molecule-amplified cell release on photoresponsive nanostructured surfaces, *ACS Appl. Mater. Interfaces*, 2019, **11**, 29681–29688.
14 D. Lu, M. Zhu, S. Wu, W. Wang, Q. Liana and B. R. Saunders, Triply responsive coumarin-based microgels with remarkably large photo-switchable swelling, *Polym. Chem.*, 2019, **10**, 2516–2526.
15 G. Cheng and J. Perez-Mercader, Dissipative self-Assembly of dynamic multicompartmentalized microsystems with light-responsive behaviors, *Chem*, 2020, **6**, 1160–1171.
16 M. Motornov, J. Zhou, M. Pita, V. Gopishetty, I. Tokarev, E. Katz and S. Minko, ''Chemical transformers'' from nanoparticle ensembles operated with logic, *Nano Lett.*, 2008, **8**, 2993–2997.
17 L. Gonzalez-Urbina, K. Baert, B. Kolaric, J. Perez-Moreno and K. Clays, Linear and nonlinear optical properties of colloidal photonic crystals, *Chem. Rev.*, 2012, **112**, 2268–2285.
18 A. H. Groschel, A. Walther, T. I. Lobling, F. H. Schacher, H. Schmalz and A. H. E. Muller, Guided hierarchical co-assembly of soft patchy nanoparticles, *Nature*, 2013, **503**, 247–251.
19 R. M. Choueiri, E. Galati, H. Thérien-Aubin, A. Klinkova, E. M. Larin, A. Querejeta-Fernández, L. Han, H. L. Xin, O. Gang, E. B. Zhulina, M. Rubinstein and E. Kumacheva, Surface patterning of nanoparticles with polymer patches, *Nature*, 2016, **538**, 79–83.
20 S. Saxena and L. A. Lyon, Enabling method to design versatile biomaterial systems from colloidal building blocks, *Mol. Syst. Des. Eng.*, 2016, **1**, 189–201.
21 K. J. McHugh, T. D. Nguyen, A. R. Linehan, D. Yang, A. M. Behrens, S. Rose, Z. L. Tochka, S. Y. Tzeng, J. J. Norman, A. C. Anselmo, X. Xu, S. Tomasic, M. A. Taylor, J. Lu, R. Guarecuco, R. Langer and A. Jaklenec, Fabrication of fillable microparticles and other complex 3D microstructures, *Science*, 2017, **357**, 1138–1142.
22 G. Chen, K. J. Gibson, D. Liu, H. C. Rees, J.-H. Lee, W. Xia, R. Lin, H. L. Xin, O. Gang and Y. Weizmann, Regioselective surface encoding of nanoparticles for programmable self-assembly, *Nat. Mater.*, 2019, **18**, 169–174.
23 F. Grillo, M. A. Fernandez-Rodriguez, M.-N. Antonopoulou, D. Gerber and L. Isa, Self-templating assembly of soft microparticles into complex tessellations, *Nature*, 2020, **582**, 219–224.
24 K. Ishihara, H. Nomura, T. Mihara, K. Kurita, Y. Iwasaki and N. Nakabayashi, Why do phospholipid polymers reduce protein adsorption?, *J. Biomed. Mater. Res.*, 1998, **39**, 323–330.
25 M. A. Dobrovolskaia and S. E. Mcneil, Immunological properties of engineered nanomaterials, *Nat. Nanotechnol.*, 2007, **2**, 469–478.
26 H. Chen, L. Yuan, W. Song, Z. K. Wu and D. Li, Biocompatible polymer materials: Role of protein-surface interactions, *Prog. Polym. Sci.*, 2008, **33**, 1059–1087.
27 N. Kamaly, Z. Y. Xiao, P. M. Valencia, A. F. Radovic-Moreno and O. C. Farokhzad, Targeted polymeric therapeutic nanoparticles: design, development and clinical translation, *Chem. Soc. Rev.*, 2012, **41**, 2971–3010.
28 H. Otsuka, Y. Nagasaki and K. Kataoka, PEGylated nanoparticles for biological and pharmaceutical applications, *Adv. Drug Delivery Rev.*, 2012, **64**, 246–255.
29 J. S. Suk, Q. Xu, N. Kim, J. Hanes and L. M. Ensign, PEGylation as a strategy for improving nanoparticle-based drug and gene delivery, *Adv. Drug Delivery Rev.*, 2016, **99**, 28–51.
30 H. Yamanaka, N. Morimoto and T. Yamaoka, Decellularization of submillimeter-diameter vascular scafolds using peracetic acid, *J. Artif. Organs*, 2020, **23**, 156–162.
31 R. Matsuno and K. Ishihara, Integrated functional nanocolloids covered with artificial cell membranes for biomedical applications, *Nano Today*, 2011, **6**, 61–74.
32 K. L. Thompson, I. Bannister, S. P. Armes and A. L. Lewis, Preparation of biocompatible sterically stabilized latexes

using well-defined poly(2-(methacryloyloxy)ethyl phosphorylcholine) macromonomers, *Langmuir*, 2010, **26**, 4693–4702.
33 Z. Shao, Y. Yang, H. Lee, J. W. Kim and C. O. Osuji, Synthesis and suspension rheology of titania nanoparticles grafted with zwitterionic polymer brushes, *J. Colloid Interface Sci.*, 2012, **386**, 135–140.
34 Y. Iwasaki and K. Ishihara, Cell membrane-inspired phospholipid polymers for developing medical devices with excellent biointerfaces, *Sci. Technol. Adv. Mater.*, 2012, **13**, 064101.
35 T. Miyata, N. Asami and T. Uragami, A reversibly antigen-responsive hydrogel, *Nature*, 1999, **399**, 766–769.
36 T. Miyata, A. Jikihara, K. Nakamae and A. S. Hoffman, Preparation of reversibly glucose-responsive hydrogels by covalent immobilization of lectin in polymer networks having pendant glucose, *J. Biomater. Sci., Polym. Ed.*, 2004, **15**, 1085–1098.
37 T. Miyata, M. Jige, T. Nakaminami and T. Uragami, Tumor marker-responsive behavior of gels prepared by biomolecular imprinting, *Proc. Natl. Acad. Sci. U. S. A.*, 2006, **103**, 1190–1193.
38 A. Kawamura, T. Kiguchi, T. Nishihata, T. Uragami and T. Miyata, Target molecule-responsive hydrogels designed by molecular imprinting using bisphenol A as a template, *Chem. Commun.*, 2014, **50**, 11101–11103.
39 C. Norioka, K. Okita, M. Mukada, A. Kawamura and T. Miyata, Biomolecularly stimuli-responsive tetra-poly(ethylene glycol) that undergoes sol–gel transition in response to a target biomolecule, *Polym. Chem.*, 2017, **8**, 6378–6385.
40 K. Matsumoto, A. Kawamura and T. Miyata, Conformationally regulated molecular binding and release of molecularly imprinted polypeptide hydrogels that undergo helix–coil transition, *Macromolecules*, 2017, **50**, 2136–2144.
41 C. Norioka, Y. Inamoto, C. Hajime, A. Kawamura and T. Miyata, A universal method to easily design tough and stretchable hydrogels, *NPG Asia Mater.*, 2021, **13**, 34.
42 S. Telitel, E. Blasco, L. D. Bangert, F. H. Schacher, A. S. Goldmann and C. Barner-Kowollik, Photo-reversible bonding and cleavage of block copolymers, *Polym. Chem.*, 2017, **8**, 4038–4042.
43 Q. Zhang, R. Li, X. Chen, X. He, A. Han, G. Fang, J. Liu and S. Wang, Study of efficiency of coupling peptides with gold nanoparticles, *Chin. J. Anal. Chem.*, 2017, **45**, 662–667.
44 G. K. Toworfe, R. J. Compostoa, I. M. Shapiro and P. Ducheyne, Nucleation and growth of calcium phosphate on amine-, carboxyl- and hydroxyl-silane self-assembled monolayers, *Biomaterials*, 2006, **27**, 631–642.
45 M. C. Munisso, A. Mahara and T. Yamaoka, Design of in situ porcine closed-circuit system for assessing blood-contacting biomaterials, *J. Artif. Organs*, 2018, **21**, 317–324.
46 Y. Liu, M. C. Munisso, A. Mahara, Y. Kambe, K. Fukazawa, K. Ishihara and T. Yamaoka, A surface graft polymerization process on chemically stable medical ePTFE for suppressing platelet adhesion and activation, *Biomater. Sci.*, 2018, **6**, 1908–1915.
47 Y. Liu, M. C. Munisso, A. Mahara, Y. Kambe and T. Yamaoka, Anti-platelet adhesion and *in situ* capture of circulating endothelial progenitor cells on ePTFE surface modified with poly(2-methacryloyloxyethyl phosphorylcholine) (PMPC) and hemocompatible peptide 1 (HCP-1), *Colloids Surf., B*, 2020, **193**, 111113.
48 H. Hayashi, M. Iijima, K. Kataoka and Y. Nagasaki, pH-Sensitive nanogel possessing reactive PEG tethered chains on the surface, *Macromolecules*, 2004, **37**, 5389–5396.
49 D. Qiu, T. Cosgrove and A. M. Howe, Narrowly Distributed Surfactant-Free Polystyrene Latex with a Water-Soluble Comonomer, *Macromol. Chem. Phys.*, 2005, **206**, 2233–2238.
50 P. B. Zetterlund, Y. Kagawa and M. Okubo, Controlled/living radical polymerization in dispersed systems, *Chem. Rev.*, 2008, **108**, 3747–3794.
51 M. Okubo, Y. Sugihara, Y. Kitayama, Y. Kagawa and H. Minami, Emulsifier-free, organotellurium-mediated living radical emulsion polymerization of butyl acrylate, *Macromolecules*, 2009, **42**, 1979–1984.
52 V. Fischer, K. Landfester and R. Muñoz-Espí, Molecularly controlled coagulation of carboxyl-functionalized nanoparticles prepared by surfactant-free miniemulsion polymerization, *ACS Macro Lett.*, 2012, **1**, 1371–1374.
53 G. B. Demirel and R. A. von Klitzing, New multiresponsive drug delivery system using smart nanogels, *Chem. Phys. Chem.*, 2013, **14**, 2833–2840.
54 Y. Xia, X. He, M. Cao, X. Wang, Y. Sun, H. He, H. Xu and J. R. Lu, Self-assembled two-dimensional thermoresponsive microgel arrays for cell growth/detachment control, *Biomacromolecules*, 2014, **15**, 4021–4031.
55 A. Darabi, J. Glasing, P. G. Jessop and M. F. Cunningham, Preparation of CO_2-switchable latexes using N-[3-(dimethylamino)propyl]-methacrylamide (DMAPMAm), *J. Polym. Sci., Part A: Polym. Chem.*, 2017, **55**, 1059–1066.
56 A. Kawamura, Y. Hata, T. Miyata and T. Uragami, Synthesis of glucose-responsive bioconjugated gel particles using surfactant-free emulsion polymerization, *Colloids Surf., B*, 2012, **99**, 74–81.
57 A. Kawamura, A. Harada, S. Ueno and T. Miyata, Weakly acidic pH and reduction dual stimuli–responsive gel particles, *Langmuir*, 2021, **37**, 11484–11492.
58 T. Cedervall, I. Lynch, S. Lindman, T. Berggård, E. Thulin, H. Nilsson, K. A. Dawson and S. Linse, Understanding the nanoparticle–protein corona using methods to quantify exchange rates and affinities of proteins for nanoparticles, *Proc. Natl. Acad. Sci. U. S. A.*, 2007, **104**, 2050–2055.
59 Y. Hoshinoa, H. Koide, K. Furuya, W. W. Haberaecker III, S. Lee, T. Kodama, H. Kanazawa, N. Oku and K. J. Shea, The rational design of a synthetic polymer nanoparticle that neutralizes a toxic peptide *in vivo*, *Proc. Natl. Acad. Sci. U. S. A.*, 2012, **109**, 33–38.
60 H. Koide, A. Okishima, Y. Hoshino, Y. Kamon, K. Yoshimatsu, K. Saito, I. Yamauchi, S. Ariizumi, Y. Zhou, T. Xiao, K. Goda, N. Oku, T. Asai and K. J. Shea, Synthetic hydrogel nanoparticles for sepsis therapy, *Nat. Commun.*, 2021, **12**, 5552.

